ORGANOMETALLICS

Article

pubs.acs.org/Organometallics

Development of Improved Amidoquinoline Polyolefin Catalysts with Ultrahigh Molecular Weight Capacity

Philip P. Fontaine* and Steve Ueligger

Performance Plastics R&D, The Dow Chemical Company, Freeport, Texas 77541, United States

Jerzy Klosin, Amaruka Hazari, Joe Daller, and Jianbo Hou

Corporate R&D, The Dow Chemical Company, 1776 Building, Midland, Michigan 48674, United States

Supporting Information

ABSTRACT: A new synthetic route to amidoquinoline olefin polymerization catalysts has been developed involving significantly less expensive and more readily available starting materials. The new methodology was used to prepare *N*-mesityl-2-methylquinolin-8-amine, which in turn was converted into trialkyl complexes of Hf, Zr, and Ti. The new complexes were characterized by elemental analysis, 1D and 2D NMR spectroscopy, and X-ray crystallography. A batch reactor ethylene/1-octene copolymerization evaluation at 140 °C showed that the new Hf congener outperformed a series of previously reported molecular olefin polymerization catalysts. In particular, the new Hf catalyst exhibits excellent activity and a remarkable capacity to produce ultrahigh molecular weight copolymers at elevated reaction temperatures.

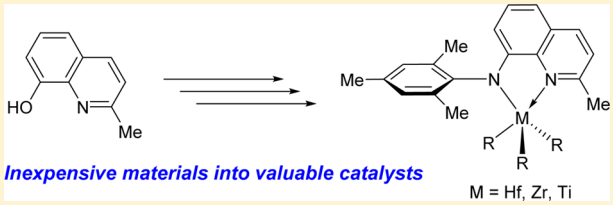

INTRODUCTION

Polyolefin catalyst families[1] that are inexpensive, easily prepared, highly active, and composed of modular frameworks have potential industrial utility. Recently, we discovered a promising new class of catalysts supported by amidoquinoline ligands,[2−4] which are a subset of a larger class of imino-amido-type catalysts[5,6] that have been extensively studied in our laboratory. Such catalysts have been used to access novel and industrially relevant polyolefin structures such as olefin block copolymers.[6f] For the Hf amidoquinoline catalysts, excellent activities were observed at elevated reaction temperatures, along with the capacity to produce extremely high molecular weight ethylene/1-octene copolymers. The thermal and chemical stability of the amidoquinoline ligands and precatalysts was another advantage, as some previously reported imino-amido catalysts were seen to be prone to isomerization, the result of which was a loss of several desirable catalyst attributes.

One drawback of the previously reported amidoquinoline complexes,[2] however, was that while the reported synthesis was relatively simple and required only two preparative steps, the raw material cost was prohibitively high for large-scale operations. Given the promising results from the initial evaluation, we sought to develop a cost-effective route to these catalysts from materials that are readily commercially available. Important structural attributes of the previously reported ligands were identified and preserved in the design of a new ligand that can be prepared via a synthetic approach that greatly reduces the material cost and maintains relative synthetic ease. Additionally, with larger quantities of the ligand precursor in hand, in addition to the Hf complex we were able to prepare Zr and Ti analogues for a comparative study. Finally, the new complexes were evaluated in a series of batch reactor ethylene/1-octene copolymerization reactions.

RESULTS AND DISCUSSION

New Synthetic Route to Ligand. The previously reported route to the representative ligand precursor is shown in Scheme 1, along with the catalogue costs and sale quantities of the raw materials. The preparation involves coupling of 8-bromo-2,4-dimethylquinoline (**1**) with 2,6-dimethylaniline (**2**), to afford the desired aminoquinoline **3** in moderate yield. A subsequent reaction of **3** with $HfBn_4$ in turn provided the precatalyst **3-HfBn$_3$** (Scheme 2). The major problem is the high cost and limited availability of **1**, for which only a single vendor was identified. Note that the unsubstituted analogue (i.e., 8-bromoquinoline) is also prohibitively expensive and similarly limited in its availability. Moreover, the resulting Hf-based polyolefin catalyst derived from 8-bromoquinoline was less efficient, displayed lower molecular weight capacity, and produced a copolymer with a broader compositional distribution, relative to that derived from **3-HfBn$_3$**.[2]

We hypothesized that the observed differences between **3-HfBn$_3$** and the analogous catalyst derived from the unsubstituted quinoline were due to the methyl substitution at the 2 position, which is in close proximity to the active site and might serve to suppress any adverse reactivity at the more activated carbon *ortho* to the quinolino nitrogen.[7] Specifically, since the polymer

Received: January 26, 2015
Published: March 31, 2015

ACS Publications © 2015 American Chemical Society

DOI: 10.1021/acs.organomet.5b00053
Organometallics 2015, 34, 1354−1363

Scheme 1. Previously Reported Route[2] to the Aminoquinoline Ligand, Including Material Costs and Quantities

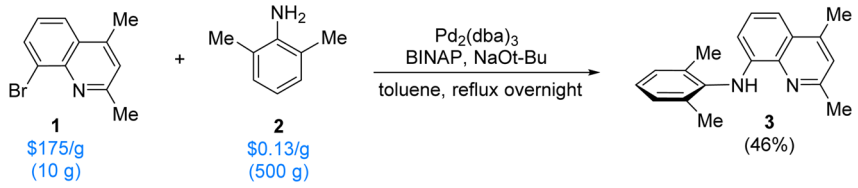

Scheme 2. Previously Reported Preparation of 3-HfBn$_3$[2]

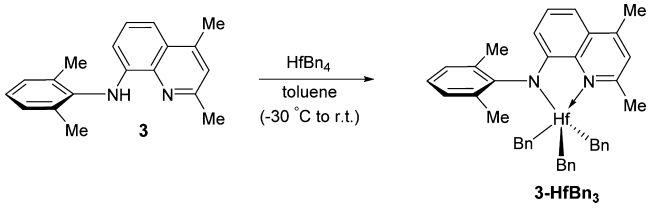

produced by **3-HfBn$_3$** had a narrower compositional distribution, we postulated that substitution at the 2-position inhibited, to some extent, the formation of a second active species. With this in mind, we looked for a less expensive starting material that retained an analogous substitution pattern. Fortunately, such a material exists, along with a literature report of its transformation to a precursor of our desired ligand target (Scheme 3). The previous report describes the conversion of 8-hydroxyquinaldine (**4**) in high yields to 8-aminoquinaldine (**5**).[8] Indeed, we found that this route is practical and amenable to large-scale preparations. We isolated **5** in 45% yield on the first attempt via column chromatography as a pale yellow solid that has moderate solubility in aliphatic hydrocarbons and excellent solubility in aromatic hydrocarbons. The reaction was very clean, and the only byproduct observed was unreacted starting material, so we believe that the yield could be easily improved (the reported literature yield is 97%, for example). With several grams of **5** in hand, however, we moved on to the next step of the synthesis without further optimization of this reaction.

The conversion of **5** into the desired aminoquinoline ligand **7** required a Pd-catalyzed coupling with an aryl bromide. Note that in this case the functionality of the substrates was the reverse of the previous route, which coupled an aniline derivative with a bromoquinoline. For the new reaction 2-bromomesitylene (**6**) was selected, as it was among the least expensive of the available aryl halides that would lead to 2,6-dimethyl substitution in the final ligand, which we deemed to be important based on the previous study.[2] The coupling proceeded smoothly, affording the desired ligand *N*-mesityl-2-methylquinolin-8-amine (**7**) as a bright yellow solid in 79% yield after column chromatography. While this new route necessitates an additional synthetic step, this is easily offset by the much lower cost and higher availability of the starting materials. For example, **4** is over 400 times less expensive than **1**. It is worth noting that **5** is also commercially available, albeit at a significantly higher cost than **4**.

As with the previously prepared aminoquinoline ligands, **7** showed appreciable solubility in hydrocarbon solvents and could be recrystallized if desired. Single crystals of **7** suitable for X-ray diffraction were obtained by slow evaporation of a toluene solution. The solid-state structure shows a planar quinolino core with an orthogonal 2,6-dimethylaniline group (Figure 1). Bond angles and distances for **7** are similar to those of **3**.[2,9]

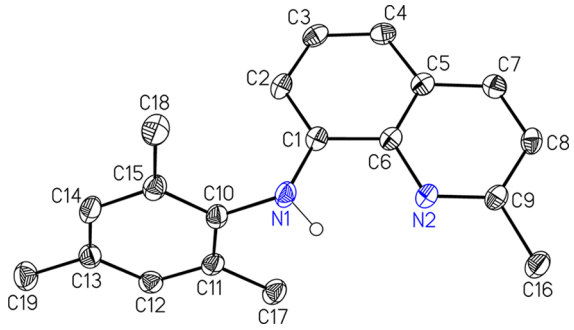

Figure 1. Molecular structure of **7**. Hydrogen atoms, except H1, are omitted for clarity. Thermal ellipsoids are shown at the 50% probability level. Selected bond lengths (Å) and angle (deg): C1−N1 = 1.3915(15), C6−N2 = 1.3652(15), C1−C6 = 1.4367(16), C1−N1−C10 120.14(19).

Scheme 3. New Route to Aminoquinoline Ligand, Including Material Costs and Quantities

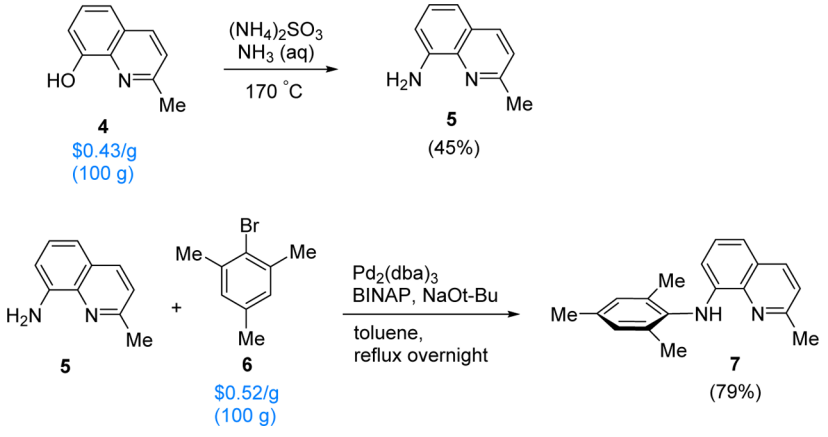

DOI: 10.1021/acs.organomet.5b00053
Organometallics 2015, 34, 1354−1363

Preparation of Metal Complexes. The ligand precursor **7** was reacted with group IV metal tetrabenzyl (MBn_4, M = Hf, Zr, Ti) compounds to furnish, in the cases of Hf and Zr, the respective amidoquinoline tribenzyl species **7-HfBn$_3$** and **7-ZrBn$_3$** (Scheme 4). The analogous chemistry did not proceed for $TiBn_4$; no reaction occurred even after several days at ambient temperature, and the thermal instability of $TiBn_4$ precluded performing this reaction at elevated temperatures. Both **7-HfBn$_3$** and **7-ZrBn$_3$** were isolated in high yields as deep red crystalline solids that have limited solubility in hexane and excellent solubility in aromatic hydrocarbons. ^{1}H NMR spectroscopy revealed fluxional behavior for both, in keeping with prior observations for amidoquinoline complexes.[2] Specifically, an exchange process that renders the three benzyl groups equivalent occurs on the NMR time scale at ambient temperature. This is evidenced by substantially broadened resonances corresponding to the protons of the benzyl groups (Figure 2). It appears that the barrier to this process is slightly lower for **7-ZrBn$_3$**, since the resonances of the benzyl groups are noticeably sharper relative to those for **7-HfBn$_3$**.

Scheme 4. Preparation of Hf and Zr Amidoquinoline Complexes

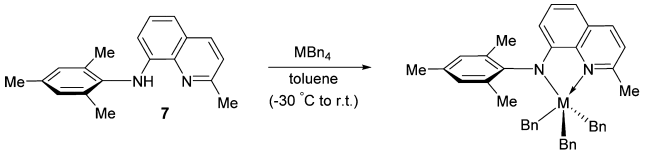

M = Hf: **7-HfBn$_3$** (95%)
M = Zr: **7-ZrBn$_3$** (88%)

The molecular structure of **7-HfBn$_3$** (Figure 3) was determined by single crystal X-ray analysis, and is similar to that of **3-HfBn$_3$**. Both adopt distorted trigonal bipyramidal geometries, with the anilino donor and two of the benzyl ligands occupying the equatorial plane. The nitrogen donors of the anionic Hf–N bonds are notably shorter in both cases, by about 0.25 Å, than the neutral quinoline nitrogen donors.

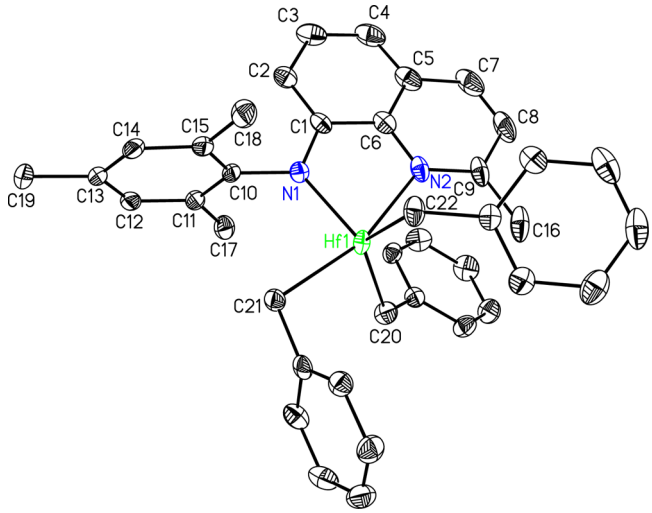

Figure 3. Molecular structure of **7-HfBn$_3$**. Hydrogen atoms are omitted for clarity. Thermal ellipsoids are shown at the 50% probability level. Selected bond lengths (Å) and angle (deg): Hf–N1 = 2.090(2), Hf–N2= 2.344(2), N1–C1 = 1.396(3), N2–C6 = 1.377(4), Hf–C20 = 2.247(3), Hf–C21 = 2.277(3), Hf–C22 =2.258(3), N1–Hf–N2 = 72.76(9).

A synthetic route to **7-TiMe$_3$** was devised using well-established literature protocols (Scheme 5).[10] Treatment of a concentrated solution of **7** with $Ti(NMe_2)_4$ at 50 °C led to the formation of **7-Ti(NMe$_2$)$_3$**. Recrystallization of the crude product from hexane at −30 °C afforded orange crystals of **7-Ti(NMe$_2$)$_3$** in 75% isolated yield. The ^{1}H NMR spectrum of **7-Ti(NMe$_2$)$_3$** at ambient temperature is indicative of the dynamic behavior of the complex in solution (Figure 4). Three separate

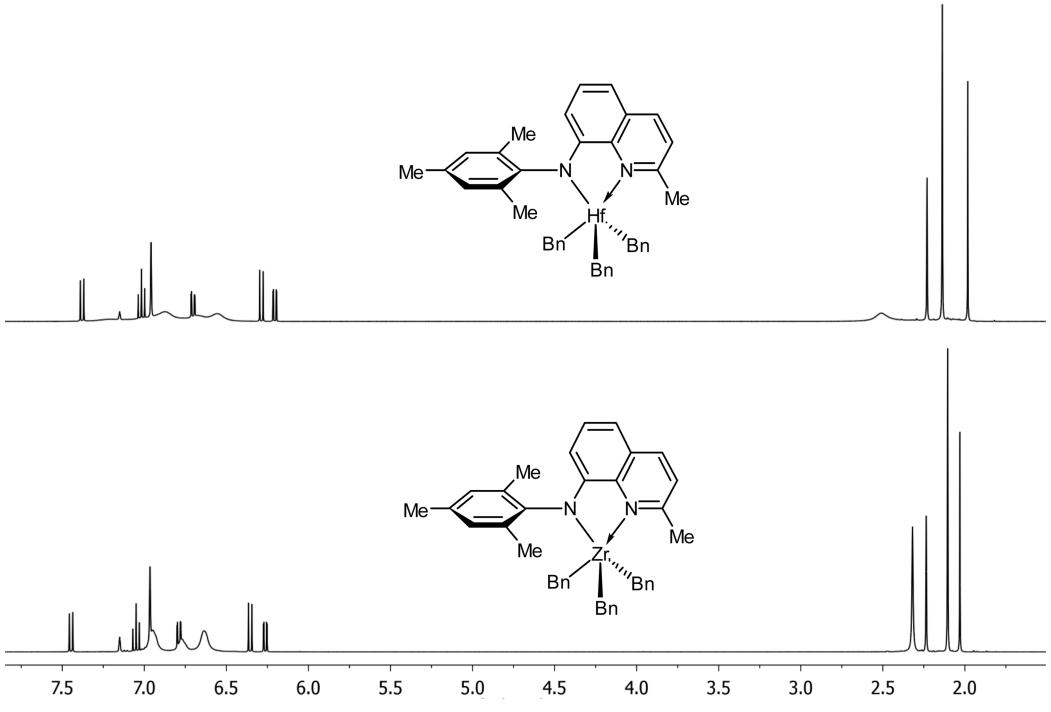

Figure 2. ^{1}H NMR spectra of **7-HfBn$_3$** and **7-ZrBn$_3$** at ambient temperature (in C_6D_6).

DOI: 10.1021/acs.organomet.5b00053
Organometallics 2015, 34, 1354–1363

Scheme 5. Preparation of Ti Amidoquinoline Complexes

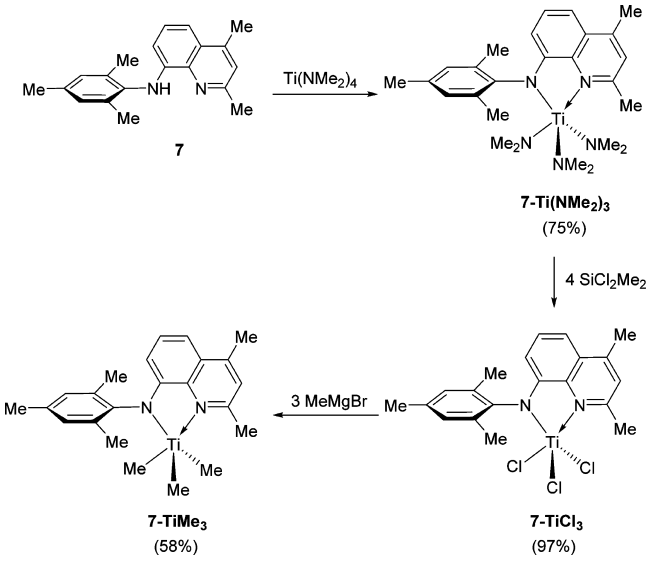

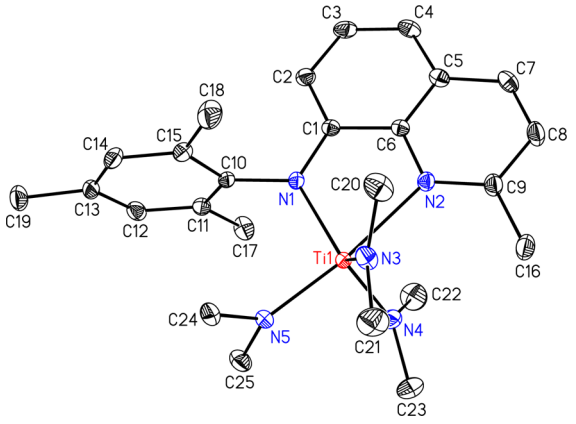

Figure 5. Molecular structure of complex 7-**Ti(NMe$_2$)$_3$**. Complex 7-**Ti(NMe$_2$)$_3$** crystallizes with four independent molecules in the unit cell. Hydrogen atoms are omitted for clarity. Thermal ellipsoids are shown at 50% probability. Selected bond lengths (Å) and angle (deg): Ti–N1= 2.0272(10), Ti–N2 = 2.3049(10), N1–C1 = 1.3800(15), N2–C6 = 1.3712(16), Ti–N3 = 1.9174(11), Ti–N4 = 1.9168(11), Ti–N5 =1.9333(11), N1–Ti–N2 = 74.42(4).

resonances corresponding to NMe$_2$ groups are observed at 3.40, 2.85, and 2.65 ppm; two of the resonances (3.40 and 2.65 ppm) are very broad, while the third resonance (2.85 ppm) remains sharp. At 75 °C, the broad resonances at 3.40 and 2.65 ppm coalesced into a single, broad peak at 3.1 ppm as a result of fast chemical exchange, while the signal at 2.85 ppm remains unchanged. The solid-state molecular structure of 7-**Ti(NMe$_2$)$_3$** (Figure 5) shows two distinctly different NMe$_2$ groups. The NMe$_2$ group in the axial position of the trigonal bipyramid has a nitrogen atom (N5) in the plane of the Ti-amidoquinoline framework with Me groups (C24/C25) (chemically equivalent) positioned above and below the ligand plane. The other two NMe$_2$ groups are in the equatorial positions of the trigonal bipyramid and are chemically equivalent; however, each contains two chemically inequivalent methyl groups. Thus, C20 is different from C21 and C22 is different from C23, while C21 and C23 (belonging to two different NMe$_2$ groups) are equivalent, as are C20 and C22. On the basis of these observations, we believe that the observed fluxional process is a result of hindered rotation along the Ti–N3 and Ti–N4 bonds, giving rise at ambient temperature to two broad resonances corresponding to C20/C22 and C21/C23 methyl groups. The sharp resonance at 2.85 ppm corresponds to the homotopic methyl groups C24 and C25. It should be stated that this exchange process is fundamentally different than the aforementioned fluxional behavior exhibited by 7-**HfBn$_3$** and 7-**ZrBn$_3$**, in which all three benzyl groups undergo chemical exchange with each other. Presumably, an analogous process could also occur for 7-**Ti(NMe$_2$)$_3$**, in which all three NMe$_2$ groups would be in chemical exchange, giving rise to one singlet in the ^{1}H NMR spectrum for all six methyl groups. We propose that the barrier for such an exchange is higher for 7-**Ti(NMe$_2$)$_3$** due to the comparative bulk of the NMe$_2$ groups relative to Bn groups, and hence at ambient temperature NMe$_2$ interconversion is in the slow exchange regime of the NMR time scale.

Treatment of 7-**Ti(NMe$_2$)$_3$** with an excess of SiMe$_2$Cl$_2$ in toluene led to the precipitation of the trichloride complex 7-

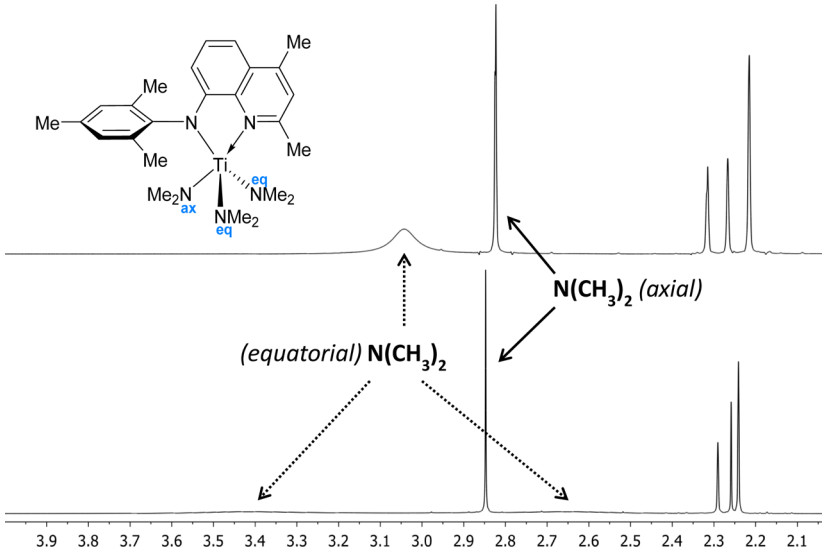

Figure 4. Portion of the ^{1}H NMR spectrum (in C$_6$D$_6$) for 7-**Ti(NMe$_2$)$_3$**, at 25 °C (bottom) and 75 °C (top).

DOI: 10.1021/acs.organomet.5b00053
Organometallics 2015, 34, 1354–1363

TiCl$_3$ as a black, crystalline solid. In the ^{1}H NMR spectrum of **7-TiCl$_3$**, the chemical shifts of the aromatic protons on the quinoline framework vary from those of the other complexes of the ligand **7** reported here. In particular, the proton *ortho* (H2) to the anilide nitrogen is significantly shifted upfield to 5.85 ppm, suggestive of increased anisotropic shielding resulting from the proximity of the arene ring coordinated to the anilide nitrogen. Conversely, the protons *para* to the anilide nitrogen and *meta* to the quinoline nitrogen are significantly shifted upfield (to 7.50 and 7.61 ppm, respectively) relative to the other complexes of **7**, indicative of the different electronic nature of the aromatic ring system for this complex. Alkylation of **7-TiCl$_3$** with three equivalents of MeMgBr afforded complex **7-TiMe$_3$** as a red, crystalline solid. The ^{1}H NMR spectrum collected at ambient temperature showed a single, slightly broad resonance at 1.81 ppm, corresponding to the three Ti-Me groups. The equivalence of the three Me groups and the broadness apparent in the resonance point to an exchange process that is analogous to that which occurs for **7-HfBn$_3$** and **7-ZrBn$_3$**. Crystals suitable for X-ray diffraction were obtained from hexane at −30 °C. Molecular structures for complexes **7-Ti(NMe$_2$)$_3$**, **7-TiCl$_3$**, and **7-TiMe$_3$**, as well as selected bond lengths and angles, are shown in Figures 5, 6, and 7, respectively. As with the Zr and Hf complexes, all three

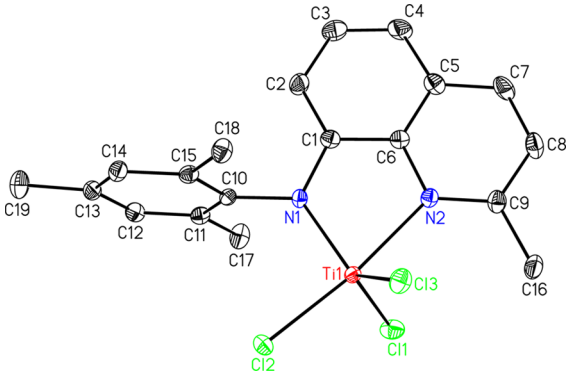

Figure 6. Molecular structure of complex **7-TiCl$_3$**. Thermal ellipsoids are shown at 50% probability. Selected bond lengths (Å) and angle (deg): Ti−N1= 1.9178(11), Ti−N2 = 2.2187(11), N2−C6 = 1.3725(16), N1−C1 = 1.4053(16), Ti−Cl1 = 2.2477(4), Ti−Cl2 = 2.2490(4), Ti−Cl3 =2.2527(4), N1−Ti−N2 = 77.89(4).

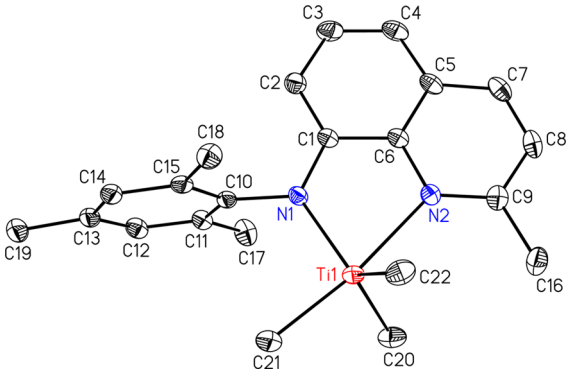

Figure 7. Molecular structure of complex **7-TiMe$_3$**. Thermal ellipsoids are shown at 50% probability. Selected bond lengths (Å) and angle (deg): Ti−N1= 1.9755(14), Ti−N2 = 2.3072(14), N1−C1 = 1.393(2), N2−C6 = 1.373(2), Ti−C20 = 2.1082(18), Ti−C21 = 2.0988(19), Ti−C22 = 2.0995(19), N1−Ti−N2 = 75.69(5).

Ti complexes display distorted trigonal bipyramidal geometry in the solid state in which the quinoline nitrogen and one of the three X-type ligands (Cl, Me, or NMe$_2$) occupy the axial positions, while the anilide nitrogen and remaining two X-type ligands occupy the equatorial positions. Throughout the series, relatively little variation is observed between the structures in terms of bond distances and angles.

Polymerization Evaluation. A series of ethylene/1-octene copolymerization runs were carried out in a 2 L batch reactor at 140 °C with a 2:1 molar ratio of 1-octene to ethylene, using [HNMe(C$_{18}$H$_{37}$)$_2$][B(C$_6$F$_5$)$_4$] as the activator. In addition to the new amidoquinoline complexes, **3-HfBn$_3$**, several previously reported imino-enamido and imino-amido catalysts, and a constrained geometry catalyst (**CGC**) were also tested for comparative purposes (Figure 8).

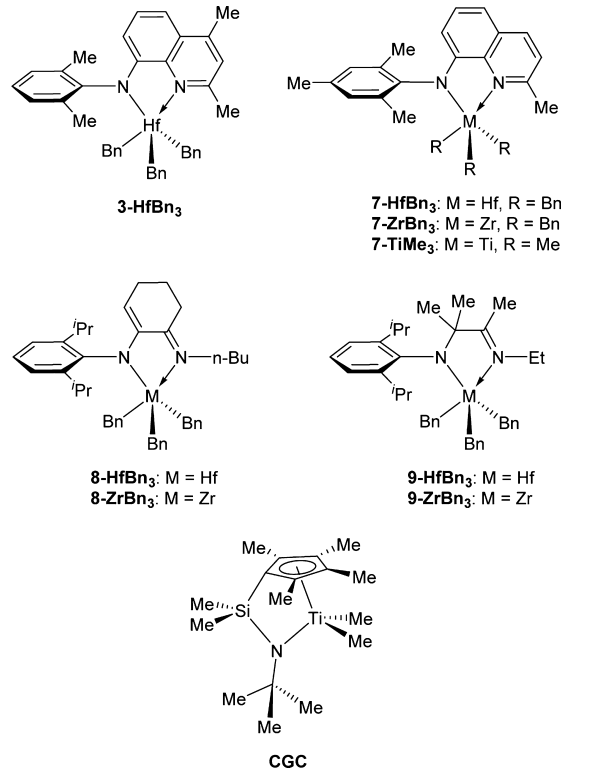

Figure 8. Complexes evaluated in polymerization reactions.

The results are shown in Table 1. A comparison of the data obtained using **3-HfBn$_3$** and **7-HfBn$_3$** reveals the similarity between the two catalysts, with the latter showing slight improvements in activity, polymer molecular weight capacity, and 1-octene incorporation. The zirconium congener **7-ZrBn$_3$** resulted in a significantly poorer catalyst in terms of both activity and molecular weight building capacity, while the titanium analogue **7-TiMe$_3$** was completely inactive under these conditions. The trends observed for the Hf and Zr congeners are similar to what has been observed previously for imino-enamido and imino-amido systems.[5] Notably, **7-HfBn$_3$** produced the copolymer with the highest molecular weight (M_w = 460 474 g/mol at 140 °C) among all the catalysts tested, an impressive feature of the new catalyst. Additionally, **7-HfBn$_3$** exhibited the highest propensity, along with **8-HfBn$_3$**, to incorporate 1-octene (13.3 mol %) among the imino-amido-type catalysts.

DOI: 10.1021/acs.organomet.5b00053
Organometallics 2015, 34, 1354−1363

Table 1. Ethylene/1-Octene Copolymerization Data at 140 °C[a]

catalyst (μmol)	poly. yield (g)	activity[b]	T_M (°C)	M_w (g/mol)	M_w/M_n	octene incorp. (mol %)[c]
3-HfBn$_3$ (0.6)	28.6	39 722	49	400 180	3.18	12.0
7-HfBn$_3$ (0.6)	33.6	46 667	45	460 474	3.38	13.3
7-ZrBn$_3$ (2.5)	18.3	6100	63	285 188	3.68	10.4
8-HfBn$_3$ (0.6)	39.9	55 417	49, 97	237 090	2.44	13.3
8-ZrBn$_3$ (2.0)	20.6	8583	65, 102	233 176	7.06	9.8
9-HfBn$_3$ (0.5)	14.3	23 833	88	64 607	2.04	7.4
9-ZrBn$_3$ (0.7)	16.1	19 167	100	113 667	8.43	4.8
CGC (0.3)	36.1	100 278	7	23 277	2.54	25.3

[a]Polymerization conditions: 140 °C, 605 g of Isopar E, 300 g of 1-octene, and 288 psi of ethylene (~42 g), precatalyst:activator = 1:1.2; activator $[HNMe(C_{18}H_{37})_2][B(C_6F_5)_4]$; precatalyst: MMAO = 1:10; reaction time 10 min. [b]Activity reported in units of grams polymer/mmol catalyst. [c]Octene content determined by ^{1}H NMR spectroscopy.

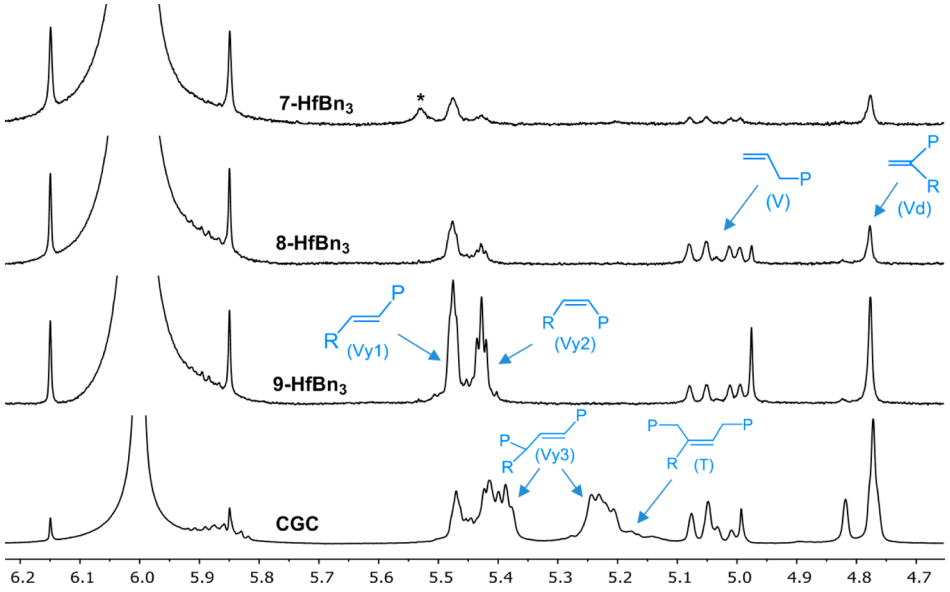

Figure 9. Fragments of ^{1}H NMR spectra of selected copolymers showing olefin region. Asterisk denotes impurity peaks resulting from polymer degradation after prolonged heating at high temperature needed for polymer dissolution.

Table 2. Mole Fractions (in ppm) of Unsaturated Groups in the Copolymers

catalyst	vinylene (*Internal, Vy3*)	trisubst'd (*Internal, T*)	vinyl (V)	vinylene (*Vy1 + Vy2*)	vinylidene (*Vd*)	total terminal unsat'n
3-HfBn$_3$	0	12	49	88	57	194
7-HfBn3	0	17	33	76	41	150
7-ZrBn$_3$	0	24	111	186	82	379
8-HfBn$_3$	0	3	113	163	59	335
8-ZrBn$_3$	0	23	291	254	99	644
9-HfBn$_3$	0	0	129	610	167	906
9-ZrBn$_3$	0	31	583	437	261	1281
CGC	935	529	290	574	552	1416

The capacity of **7-HfBn$_3$** to produce ultrahigh polymer molecular weights at elevated temperatures, and with good catalytic activity, is an attractive feature of this new catalyst. Generally speaking, molecular weight building capacity is a very valuable characteristic of molecular polyolefin catalysis, especially at elevated temperatures. In order to gain a more detailed understanding of this promising new catalyst, we carried out end group analyses on the copolymers obtained in this study. Such analysis can provide detailed information about the catalyst behavior, specifically with regard to the termination events.[11] For polymerization runs conducted without hydrogen as a molecular weight control agent, chain termination results in terminal unsaturation for every polymer chain, and, as such, the total amount of chain end unsaturation is directly related to the catalyst molecular weight building capacity. Additionally, the type of (terminal) unsaturation is determined by the specifics of the termination mechanism; for example, termination after an ethylene insertion results in a vinyl end group, whereas termination after an α-olefin insertion leads to a vinlyene (following a 2,1-insertion) or a vinylidene (following a 1,2-insertion). The types and various amounts of these unsaturations can directly impact the resulting polymer architecture and properties; for example, the influence of vinyl groups' concentration on long-chain branching formation is well established.[12] For the copolymers generated in this study, a striking detail is the variation in the amount of total terminal

DOI: 10.1021/acs.organomet.5b00053
Organometallics 2015, 34, 1354−1363

unsaturations, which as expected trended with copolymer molecular weight determined by GPC. The copolymer with the lowest molecular weight (M_w = 23 277 g/mol made by **CGC**) showed the highest number of terminal unsaturations (1416 ppm), while the copolymer (M_w = 460 474 g/mol) made by **7-HfBn$_3$** had almost an order of magnitude lower level of unsaturation (150 ppm). The relative distribution of unsaturation types was similar among all copolymers derived from imino-amido, imino-enamido, and amidoquinoline catalysts (Figure 9, Table 2), with the main difference being the level of unsaturation. For the copolymer made by **7-HfBn$_3$**, the intensities of the vinyl, vinylene, and vinylidene end groups were lower relative to all the other catalysts, indicating higher termination barriers following both ethylene and octene (1,2 and 2,1) insertions for this catalyst. In contrast to **CGC**, all the imino-amido-type catalysts produced very small amounts of internal unsaturations (Vy3, T).

SUMMARY

A new synthetic route to amidoquinoline ligands has been developed involving significantly less expensive and more readily available starting materials. The new methodology was used to prepare *N*-mesityl-2-methylquinolin-8-amine (**7**), which in turn was reacted with Hf and Zr tetrabenzyl precursors, affording the respective tribenzyl compounds **7-HfBn$_3$** and **7-ZrBn$_3$** in excellent yields. The analogous trialkyl Ti complex, **7-TiMe$_3$**, was synthesized via chlorination and subsequent alkylation of **7-Ti(NMe$_2$)$_3$**. The new complexes were characterized by NMR spectroscopy and X-ray crystallography.

A batch reactor ethylene/1-octene copolymerization evaluation showed that **7-HfBn$_3$** compared favorably to previously reported amidoquinoline catalysts and outperformed many of the previously reported imino-amido-based catalysts. The new catalyst derived from **7-HfBn$_3$** exhibited excellent activity and an impressive capacity to produce ultrahigh molecular weight copolymers. The discovery of advantaged catalysts such as **7-HfBn$_3$** that can be easily prepared in a few steps from inexpensive and readily available materials is an important goal within the industrial polyolefin community and remains a research focus in our laboratory.

EXPERIMENTAL SECTION

General Considerations. All reagents and solvents were obtained from commercial sources and used directly, unless otherwise noted. Toluene and hexane were degassed and dried over alumina prior to use. Air-sensitive manipulations were performed in a Vacuum Atmospheres inert atmosphere glovebox under a dry nitrogen atmosphere or by using standard Schlenk and vacuum line techniques. NMR spectra were recorded on Bruker Avance-400 and Varian Mercury-400 spectrometers. ^{1}H NMR data are reported as follows: chemical shift (integration, multiplicity (br = broad, s = singlet, d = doublet, t = triplet, q = quartet, p = pentet, and m = multiplet), and assignment). Chemical shifts for ^{1}H NMR data are reported in ppm downfield from internal tetramethylsilane (TMS, δ scale) using residual protons in the deuterated solvent (C_6D_6, 7.15 ppm; toluene-d_8, 2.09 ppm) as references. ^{13}C NMR data were determined with ^{1}H decoupling, and the chemical shifts are reported in ppm vs tetramethylsilane (C_6D_6, 128.1 ppm; toluene-d_8, 20.4 ppm). Elemental analyses were performed at Midwest Microlab, LLC. High-resolution mass spectroscopy (HRMS) analyses were carried out using flow injection (0.5 mL of 50/50 v/v% of 0.1% formic acid in water/THF) on an Agilent 6520 quadrupole-time-of-flight MS system via a dual-spray electrospray interface operating in the positive ion mode.

*Preparation of 2-Methylquinolin-8-amine (**5**).* A 100 mL Parr reactor was charged with **4** (10.0 g, 62.8 mmol), $(NH_4)_2SO_3{\cdot}H_2O$ (16.9 g, 126 mmol), and aqueous ammonia solution (32%, 50 mL). The resulting mixture was heated to 170 °C for 2 days, at which point the contents were drained out, rinsing with water (100 mL). This mixture was extracted with CH_2Cl_2 (3 × 50 mL), and the combined organic extracts were dried over $MgSO_4$. NMR analysis showed partial conversion to the desired material and unreacted starting material. Rather than continuing the reaction, the mixture was purified at this point via column chromatography on silica gel, eluting with 1:1 CH_2Cl_2/hexane, affording **5** as a yellow solid (4.50 g, 45%). Spectroscopic data were consistent with the published data.[8]

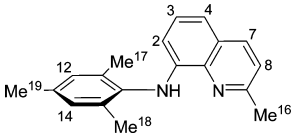

*Preparation of N-Mesityl-2-methylquinolin-8-amine (**7**).* A round-bottomed flask equipped with a reflux condenser was charged with $Pd_2(dba)_3$ (0.72 g, 0.79 mmol), *rac*-BINAP (1.08 g, 1.74 mmol), and sodium *tert*-butoxide (2.13 g, 22.1 mmol) in toluene (75 mL). To the resulting suspension were added **5** (2.50 g, 15.8 mmol) and **6** (3.73 g, 15.8 mmol). The mixture was heated under reflux overnight and then pumped down to dryness under vacuum. The crude residue was purified by flash column chromatography eluting with 5% EtOAc in hexane. The product was dried under vacuum, affording **7** as a bright yellow solid (3.45 g, 79%). ^{1}H NMR (C_6D_6): 7.76 (1H, s, N*H*); 7.58 (1H, d, $^3J_{H-H}$ = 8.4 Hz, *H7*), 7.13 (1H, dd, $^3J_{H-H}$ = 8.1, 7.6 Hz, *H3*), 6.95 (1H, dd, $^3J_{H-H}$ = 8.1 Hz, $^4J_{H-H}$ = 1.2 Hz, *H4*), 6.85 (2H, m, *H12, H14*); 6.80 (1H, d, $^3J_{H-H}$ = 8.4 Hz, *H8*), 6.41 (1H, dd, $^3J_{H-H}$ = 7.6 Hz, $^4J_{H-H}$ = 1.2 Hz, *H2*), 2.51 (3H, s, *Me*$_{16}$), 2.18 (3H, s, *Me*$_{19}$), 2.17 (6H, s, *Me*$_{17,18}$). ^{13}C{^{1}H} NMR (C_6D_6): 156.0, 143.7, 138.4, 137.2, 136.7, 136.6, 136.01, 129.96, 127.8, 127.6, 122.5, 115.1, 106.6, 25.5, 21.4, 18.7. ES-HRMS (*m*/*e*): calcd for $C_{21}H_{24}N_2$ $(M + H)^+$ 277.1705, found 277.1706.

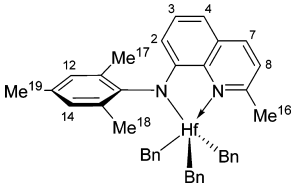

*Preparation of (Mesityl(2-methylquinolin-8-yl)amino)-tribenzylhafnium (**7-HfBn$_3$**).* A solution of **7** (0.285 g, 1.03 mmol) in toluene (5 mL) was cooled to −30 °C, then added to a vial containing $HfBn_4$ (0.528 g, 0.973 mmol). The resulting solution turned orange immediately and was allowed to warm to ambient temperature and stirred for 0.5 h. The volume of toluene was reduced to ca. 2 mL, and hexane (ca. 8 mL) was added, at which point the solution was cooled to −30 °C. After 1 day, the resulting orange crystals were collected and dried under vacuum, affording the desired product in high purity (0.67 g, 95%). Anal. Calcd for $C_{40}H_{40}HfN_2$: C, 66.06; H, 5.54; N, 3.85. Found: C, 66.16; H, 5.49; N, 3.78. ^{1}H NMR (C_6D_6): 7.38 (1H, d, $^3J_{H-H}$ = 8.4 Hz, *H7*), 7.02 (1H, dd, $^3J_{H-H}$ = 8.1, 7.8 Hz, *H3*), 6.96 (2H, m, *H12, H14*), 6.88 (6H, br, Hf-*Bn*), 6.70 (1H, dd, $^3J_{H-H}$ = 8.1 Hz, $^4J_{H-H}$ = 1.1 Hz, *H4*), 6.67 (3H, br, Hf-*Bn*), 6.56 (6H, br, Hf-*Bn*), 6.29 (1H, d, $^3J_{H-H}$ = 8.4 Hz, *H8*), 6.20 (1H, dd, $^3J_{H-H}$ = 7.8 Hz, $^4J_{H-H}$ = 1.1 Hz, *H2*), 2.51 (6H, br, Hf-*Bn*), 2.23 (3H, s, *Me*$_{19}$), 2.14 (6H, s, *Me*$_{17,18}$), 1.98 (3H, s, *Me*$_{16}$). ^{13}C{^{1}H} NMR (C_6D_6): 159.6, 151.7, 147.0 (br), 144.1, 140.9, 139.5, 135.8, 135.3, 130.8, 129.6, 128.3 (br), 128.1, 127.9 (br), 123.8, 122.6 (br), 115.7, 111.2, 89.9 (br), 25.8, 21.4, 19.0.

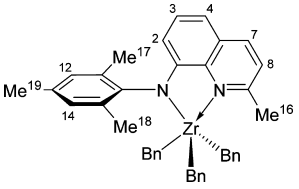

DOI: 10.1021/acs.organomet.5b00053
Organometallics 2015, 34, 1354−1363

*Preparation of (Mesityl(2-methylquinolin-8-yl)amino)-tribenzylzirconium (**7-ZrBn$_3$**).* A solution of 7 (0.285 g, 1.03 mmol) in toluene (5 mL) was cooled to −30 °C, then added to a vial containing $ZrBn_4$ (0.443 g, 0.973 mmol). The resulting solution turned deep red immediately and was allowed to warm to ambient temperature and stirred for 0.5 h. The volume of toluene was reduced to ca. 2 mL, and hexane (ca. 8 mL) was added, at which point the solution was cooled to −30 °C. After 1 day, the resulting deep red crystals were collected and dried under vacuum, affording the desired product in high purity (0.62 g, 88%). Anal. Calcd for $C_{40}H_{40}ZrN_2$: C, 75.07; H, 6.30; N, 4.38. Found: C, 74.86; H, 6.25; N, 4.49. ^{1}H NMR (C_6D_6): 7.45 (1H, d, $^3J_{H-H}$ = 8.3 Hz, *H7*), 7.05 (1H, dd, $^3J_{H-H}$ = 8.0, 7.8 Hz, *H3*), 6.97 (2H, m, *H12, H14*), 6.95 (6H, br, Hf-*Bn*), 6.79 (1H, dd, $^3J_{H-H}$ = 8.0 Hz, $^4J_{H-H}$ = 1.1 Hz, *H4*), 6.77 (3H, br, Hf-*Bn*), 6.64 (6H, br, Hf-*Bn*), 6.36 (1H, d, $^3J_{H-H}$ = 8.3 Hz, *H8*), 6.26 (1H, dd, $^3J_{H-H}$ = 7.8 Hz, $^4J_{H-H}$ = 1.1 Hz, *H2*), 2.32 (6H, br, Hf-*Bn*), 2.24 (3H, s, Me_{19}), 2.10 (6H, s, $Me_{17,18}$), 2.03 (3H, s, Me_{16}). ^{13}C{^{1}H} NMR (C_6D_6): 158.6, 152.1, 147.2 (br), 146.3, 140.5, 139.5, 135.3, 134.7, 130.7, 129.7 (br), 129.5, 127.7 (br), 123.9, 122.8 (br), 115.4, 110.1, 77.7 (br), 26.4, 21.4, 19.3.

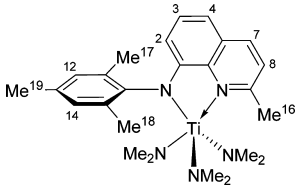

*Preparation of (Mesityl(2-methylquinolin-8-yl)amino)tris-(dimethylaminato)titanium (**7-Ti(NMe$_2$)$_3$**).* To a solution of 7 (2.536 g, 9.2 mmol) dissolved in 10 mL of warm (60 °C) hexane was added $Ti(NMe_2)_4$ (2.057 g, 9.2 mmol). The reaction mixture was heated at 65 °C. Within 30 min, the solution became deep red. After stirring for 22 h at 65 °C, the resulting hazy solution was filtered. Upon filtration, large crystals started to form. After 1 h at ambient temperature, the vial was put into the freezer for 5 h (−30 °C). Crystals were collected on a frit, washed with 2 mL of cold (−30 °C) hexane, and dried under reduced pressure to produce 3.125 g of product. Yield: 75%. Anal. Calcd for $C_{25}H_{37}N_5Ti$: C, 65.93; H, 8.19; N, 15.38. Found: C, 66.20; H, 7.86; N, 15.01. ^{1}H NMR (500 MHz, C_6D_6): δ 7.59 (1H, d, $^3J_{H-H}$ = 8.3 Hz, *H7*), 7.14 (1H, t, $^3J_{H-H}$ = 7.9 Hz, *H3*), 7.05 (2H, m, *H12, H14*), 6.85 (1H, dd, $^3J_{H-H}$ = 7.9, $^4J_{H-H}$ = 1.1 Hz, *H4*), 6.76 (1H, d, *J* = 8.3 Hz, *H8*), 6.18 (1H, dd, dd, $^3J_{H-H}$ = 7.9, $^4J_{H-H}$ = 1.1 Hz, *H2*), 3.60−3.20 (6H, br s, Ti-$N_{eq}(CH_3)$) 2.86 (6H, s, Ti-$N_{ax}(CH_3)_2$), 2.80−2.50 (6H, br s, Ti-$N_{eq}(CH_3)$), 2.30 (3H, s, Me_{19}), 2.27 (3H, s, Me_{16}), 2.25 (6H, s, $Me_{17,18}$). ^{13}C NMR (126 MHz, C_6D_6): δ 156.33, 153.64, 146.92, 139.77, 138.10, 133.01, 132.34, 129.33, 129.19, 127.91, 123.15, 113.06, 106.55, 48.03, 45.37 (br), 22.01, 21.08, 21.06, 18.66.

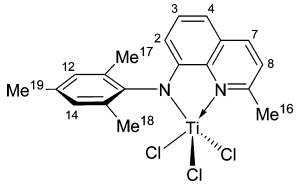

*Preparation of (Mesityl(2-methylquinolin-8-yl)amino)-trichlorotitanium (**7-TiCl$_3$**).* To complex 7-**Ti(NMe$_2$)$_3$** (2.976 g, 6.5 mmol) dissolved in 8 mL of toluene was added $SiMe_2Cl_2$ (3.373 g, 26.1 mmol), resulting in a sudden color change of the solution from orange-red to brown. After 10 min of stirring at ambient temperature, highly crystalline product (brown-black) appeared. After stirring for 3 h at ambient temperature, 10 mL of hexane was added and the suspension was placed in the freezer for 3 h. A crystalline solid was collected on a frit, and it was washed with cold hexane (2 × 3 mL) and dried under reduced pressure to give 2.716 g of product. Yield: 97%. Anal. Calcd for $C_{19}H_{19}N_2Ti$: C, 53.12; H, 4.46; N, 6.52. Found: C, 52.82; H, 4.53; N, 6.24. ^{1}H NMR (500 MHz, CD_2Cl_2): δ 8.40 (1H, d, $^3J_{H-H}$ = 8.4 Hz, *H7*), 7.61 (1H, d, $^3J_{H-H}$ = 8.4 Hz, *H8*), 7.50 (1H, dd, $^3J_{H-H}$ = 8.0, $^4J_{H-H}$ = 1.1 Hz, *H4*), 7.36 (1H, t, *J* = 7.9 Hz, *H3*), 7.08−7.03 (2H, m, *H12, H14*), 5.83 (dd, $^3J_{H-H}$ = 7.7, $^4J_{H-H}$ = 1.1 Hz, *H2*), 3.13 (3H, s, Me_{16}), 2.38 (3H, d, $^4J_{H-H}$ = 0.7 Hz, Me_{19}), 2.28 (6H, d, $^4J_{H-H}$ = 0.7 Hz, $Me_{17,18}$). ^{13}C NMR (126 MHz, CD_2Cl_2): δ 160.26, 156.75, 147.72, 141.01, 139.82, 138.49, 130.07, 129.39, 128.54, 128.04, 125.70, 122.85, 108.58, 25.67, 21.17, 18.45.

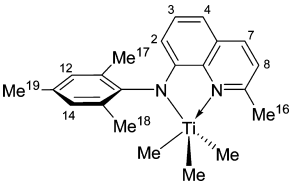

*Preparation of (Mesityl(2-methylquinolin-8-yl)amino)-trimethyltitanium (**7-TiMe$_3$**).* To 7-**TiCl$_3$** (0.681 g, 1.59 mmol) dissolved in 15 mL of toluene was added 1.69 mL (5.07 mmol) of a 3 M diethyl ether solution of MeMeBr, giving a deep red solution. The reaction mixture was stirred for 1 h at ambient temperature. The solvent was removed from the reaction mixture under reduced pressure. To the residue was added 40 mL of hexane. After stirring for 5 min at ambient temperature, the suspension was filtered, giving a red filtrate that was put into the freezer (−30 °C). The supernatant was decanted from the chilled filtrate, affording large red crystals, which were washed with 2 mL of cold hexane and then dried under reduced pressure to give 0.158 g of product (first crop). NMR spectroscopy showed the clean formation product. The supernatant was dried under reduced pressure, leaving a red, crystalline solid. To this residue was added 8 mL of hexane, which partly dissolved the residue. This suspension was put into the freezer (−30 °C) for 3 days. The supernatant was decanted from a red, crystalline solid that was washed with 1 mL of cold hexane and then dried under reduced pressure to give 0.182 g of product (second crop). NMR showed clean product. Combined yield: 0.340 g, 58%. Anal. Calcd for $C_{22}H_{28}N_2Ti$: C, 71.74; H, 7.61; N, 7.61. Found: C, 71.51; H, 7.38; N, 7.46. ^{1}H NMR (400 MHz, C_6D_6): δ 7.41 (1H, d, $^3J_{H-H}$ = 8.4 Hz, *H7*), 7.07 (1H, t, $^3J_{H-H}$ = 7.9 Hz, *H3*), 7.01 (2H, h, $^4J_{H-H}$ = 0.7 Hz, *H12, H14*), 6.78 (1H, dd, $^3J_{H-H}$ = 8.0, $^4J_{H-H}$ = 1.0 Hz, *H4*), 6.51 (1H, d, *J* = 8.4 Hz, *H8*), 6.27 (1H, dd, $^3J_{H-H}$ = 7.8, $^4J_{H-H}$ = 1.1 Hz, *H2*), 2.49 (3H, s, Me_{16}), 2.37 (6H, s, $Me_{17,18}$), 2.25 (3H, s, Me_{19}), 1.81 (br s, 9H, Ti-*Me*). ^{13}C NMR (101 MHz, C_6D_6): δ 156.84, 151.90, 146.85, 139.22, 138.90, 134.96, 133.71, 130.01, 129.08, 127.65, 123.43, 115.00, 107.61, 70.21 (br), 24.38, 21.12, 18.68.

Structure Determination. X-ray intensity data were collected on a Bruker SMART diffractometer using Mo Kα radiation (λ = 0.710 73 Å) and an APEXII CCD area detector. Raw data frames were read by the SAINT[13] program and integrated using 3D profiling algorithms. The resulting data were reduced to produce *hkl* reflections and their intensities and estimated standard deviations. The data were corrected for Lorentz and polarization effects, and numerical absorption corrections were applied based on indexed and measured faces. The structures were solved and refined in SHELXTL6.1, using full-matrix least-squares refinement. The non-H atoms were refined with anisotropic thermal parameters, and all of the H atoms were calculated in idealized positions and refined riding on their parent atoms. The refinement was carried out using F^2 rather than *F* values. R_1 is calculated to provide a reference to the conventional *R* value, but its function is not minimized.

*Structure **7**.* $C_{19}H_{20}N_2$, M_w = 276.37, triclinic, $P\bar{1}$ (0.210 × 0.160 × 0.130 mm^3), *a* = 7.1032(2) Å, *b* = 8.6182(2) Å, *c* = 12.4141(4) Å, α = 98.911(2)°, β = 90.099(2)°, γ = 91.834(2)°, temp = 100(2) K, *Z* = 2, *V* = 750.38(4) Å^3, R1 = 0.0431, 0.0544, wR2 = 0.1154, 0.1226 ($I > 2\sigma(I)$, all data), GOF = 1.070.

*Structure **7-HfBn$_3$**.* $C_{80}H_{75}Hf_2N_4$, M_w = 1449.42, monoclinic, $P2_1/c$ (0.160 × 0.130 × 0.090 mm^3), *a* = 20.9081(3) Å, *b* = 18.6828(3) Å, *c* = 18.2982(3) Å, β = 112.6890(10)°, temp = 100(2) K, *Z* = 4, *V* = 6594.53(18) Å^3, R1 = 0.0262, 0.0400, wR2 = 0.0533, 0.0575 ($I > 2\sigma(I)$, all data), GOF = 1.029.

*Structure **7-Ti(NMe$_2$)$_3$**.* $C_{100}H_{148}N_{20}Ti_4$, 1821.98, triclinic, $P\bar{1}$ (0.420 × 0.260 × 0.240 mm^3), *a* = 13.9968(2) Å, *b* = 1814.0744(2) Å, *c* = 26.3453(5) Å, α = 91.5480(10)°, β = 96.0730(10)°, γ = 101.1860(10)°,

DOI: 10.1021/acs.organomet.5b00053
Organometallics 2015, 34, 1354−1363

temp = 100(2) K, Z = 8, V = 5056.75(14) Å^3, R1 = 0.0334, 0.0401, wR2 = 0.0906, 0.0956 ($I > 2\sigma(I)$, all data), GOF = 1.05.

Structure ***7-TiCl$_3$***. $C_{25}H_{25}Cl_3N_2Ti$, 507.72, triclinic, $P\bar{1}$ (0.350 × 0.280 × 0.240 mm^3), a = 10.1358(2) Å, b = 11.3270(3) Å, c = 11.8363(3) Å, α = 69.3490(10)°, β = 75.1330(10)°, γ = 80.5650(10)°, temp = 100(2) K, Z = 2, V = 1224.96(5) Å^3, R1 = 0.0251, 0.0286, wR2 = 0.0634, 0.066 ($I > 2\sigma(I)$, all data), GOF = 1.045.

Structure ***7-TiMe$_3$***. $C_{22}H_{28}N_2Ti$, 368.36, triclinic, $P\bar{1}$ (0.270 × 0.140 × 0.090 mm^3), a = 11.7159(2) Å, b = 12.8671(2) Å, c = 14.0049(2) Å, α = 104.0544(11)°, β = 96.1202(11)°, γ = 97.9432(11)°, temp = 100(2) K, Z = 4, V = 2006.68(6) Å^3, R1 = 0.0391, 0.0597, wR2 = 0.0933, 0.1025 ($I > 2\sigma(I)$, all data), GOF = 1.029.

Batch Reactor Ethylene/1-Octene Copolymerizations. Polymerization reactions were carried out at 140 °C. While the reactor was reaching polymerization temperature, 10 μmol of MMAO was added to the reactor as a scavenger for trace O_2 and water. A 2 L Parr reactor was used in the polymerizations. All feeds were passed through columns of alumina and Q-5 catalyst (available from Engelhard Chemicals Inc.) prior to introduction into the reactor. Precatalyst and activator ($[HNMe(C_{18}H_{37})_2][B(C_6F_5)_4]$, obtained from Boulder Scientific Co.) solutions were handled in a nitrogen-filled glovebox. A stirred 2 L reactor was charged with approximately 605 g of mixed alkanes solvent and 300 g of 1-octene comonomer. Once at temperature, the reactor was saturated with ethylene at 288 psig (1.99 MPa). Precatalysts were mixed with the activator, as dilute solutions in toluene, and transferred to a catalyst addition tank and injected into the reactor. The polymerization conditions were maintained for 10 min with ethylene added on demand. Heat was continuously removed from the reaction vessel through an internal cooling coil. The resulting solution was removed from the reactor, quenched with isopropyl alcohol, and stabilized by addition of 10 mL of a toluene solution containing approximately 67 mg of a hindered phenol antioxidant (Irganox 1010 from Ciba Geigy Corporation) and 133 mg of a phosphorus stabilizer (Irgafos 168 from Ciba Geigy Corporation). Between polymerization runs, a wash cycle was conducted in which 850 g of mixed alkanes was added to the reactor, and the reactor was heated to 160 °C. The reactor was then emptied of the heated solvent immediately before beginning a new polymerization run. Polymers were recovered by drying for about 12 h in a temperature-ramped vacuum oven with a final set point of 140 °C. Note that the catalyst activities were determined using the resulting polymer yields, relative to the amount of precatalyst injected. The amount of catalyst, in turn, was varied in accord with its activity. Specifically, it was necessary to add enough of each precatalyst to obtain sufficient quantities of the copolymer products for analytical measurements. Conversely, it was also desired to maintain temperature control of the exothermic polymerization reactions (the polymerization exotherms were kept to less than 5 °C for all runs), and so it was not feasible to inject an arbitrary amount of the precatalysts. Additionally, catalyst activity can be significantly impacted by the presence of impurities; therefore, comparison of the catalyst control (CGC) to historical data was used to ensure the proper performance of the reactor. The data presented herein correspond to single runs with the indicated catalysts. From the historical data with CGC, we estimate the variation in catalyst activity on a given day is ±10%. Likewise, the variation in the resulting polymer molecular weight and octene incorporation data is typically ±10%, while the variation in the polymer melting temperatures is ±2 °C.

Polymer Characterization. Melting (T_m) temperatures of polymers were measured by differential scanning calorimetry (Q2000 DSC, TA Instruments, Inc.). Samples were first heated from ambient temperature to 200 °C using the "Jump To" feature. After being held at this temperature for 4 min, the samples were cooled to −90 °C at 10 °C/min, held for 4 min, and then heated again to 200 °C. Molecular weight distribution (M_w, M_n) information was determined by analysis on a custom Dow-built robotic-assisted dilution high-temperature gel permeation chromatographer (RAD-GPC). Polymer samples were dissolved for 90 min at 160 °C at a concentration of 5−7 mg/mL in 1,2,4-trichlorobenzene (TCB) stabilized by 300 ppm of BHT in capped vials while stirring. They were then diluted to 1 mg/mL immediately before a 400 μL aliquot of the sample was injected. The GPC utilized two Polymer Laboratories PL gel 10 μm MIXED-B columns (300 mm × 10 mm) at a flow rate of 2.0 mL/min at 150 °C. Sample detection was performed using a PolyChar IR4 detector in concentration mode. A conventional calibration of narrow polystyrene (PS) standards was utilized, with apparent units adjusted to homopolyethylene (PE) using known Mark−Houwink coefficients for PS and PE in TCB at this temperature. To determine octene incorporation, polymer samples were dissolved at a concentration of 30 mg/mL in 1,2,4-trichlorobenzene at 160 °C for 1 h while shaking. A 100 μL aliquot of each polymer/TCB solution was deposited into individual cells on a custom silicon wafer at 160 °C under inert nitrogen atmosphere. The wafer was held at 160 °C for 45 min and then pulled from the heat and allowed to cool to ambient temperature. The wafer was then analyzed using a Nicolet Nexus 670 FT-IR ESP infrared spectrometer. Octene incorporation was determined by ^{1}H NMR spectroscopy. Typically, 0.055 g of the respective copolymer sample was cut into pieces and transferred into an 8 mm NMR tube, followed by adding approximately 1.6 mL of 1,1,2,2-tetrachloroethane-d_2 (TCE) containing 1 mM Cr(acac)$_3$. The sample tube was then purged with nitrogen, sealed with a piece of Teflon tape, and heated at 110 °C using a heating block. The tube was vortexed repeatedly to ensure sample homogeneity prior to any NMR measurement. Subsequent ^{1}H NMR experiments were performed on a Bruker AVANCE 600 MHz spectrometer equipped with a 10 mm probe. For each sample, two types of experiments were conducted. A standard single-pulse ^{1}H experiment was performed first to quantify the peak ratio of polymer to solvent. The second experiment employed the ^{1}H presaturation sequence using a continuous wave to suppress the polymer backbone peak. The level of octane was quantified by referencing the unsaturated CH_3 signal to the same solvent peak. All measurements were performed at 110 °C with no sample spinning using the following parameters: 90° pulse of 26.5 μs, 2.7 s acquisition time, 2 s presaturation time (pw = 0.24 mW), 15 s total repetition time, 16 scans for standard spectra, and 128−256 scans for presaturated spectra. The spectra were centered at 1.296 ppm with a spectrum width of 20 ppm. The obtained ^{1}H spectra were referenced to the TCE solvent peak at 6.0 ppm (residual protonated solvent).

■ ASSOCIATED CONTENT

Supporting Information

NMR spectra (1D and 2D) and X-ray data (including CIF files) for all new compounds and tabulated NMR data for polymer analyses are included. This material is available free of charge via the Internet at http://pubs.acs.org.

■ AUTHOR INFORMATION

Corresponding Author

*E-mail: PFontaine@dow.com.

Notes

The authors declare no competing financial interest.

■ REFERENCES

(1) For reviews on postmetallocene molecular polyolefin catalyst familes, see: (a) Britovsek, G. J. P.; Gibson, V. C.; Wass, D. F. *Angew. Chem., Int. Ed.* **1999**, *38*, 428−447. (b) Gibson, V. C.; Spitzmesser, S. K. *Chem. Rev.* **2003**, *103*, 283−316. (c) Lamberti, M.; Mazzeo, M.; Pappalardo, D.; Zambelli, A.; Pellecchia, C. *Macromol. Symp.* **2004**, *213*, 235−252. (d) Busico, V. *Macromol. Chem. Phys.* **2007**, *208*, 26−29. (e) Baier, M. C.; Zuideveld, M. A.; Mecking, S. *Angew. Chem., Int. Ed.* **2014**, *53*, 2−25.

(2) Fontaine, P. P.; Klosin, J.; McDougal, N. *Organometallics* **2012**, *31*, 6244−6251.

(3) For selected examples of metal complexes ligated by aminoquinoline ligands, see: (a) Lee, J. C.; Muller, B.; Pregosin, P.; Yap, G. P. A.; Rheingold, A. L.; Crabtree, R. H. *Inorg. Chem.* **1995**, *34*, 6295−6301. (b) Peters, J. C.; Harkins, S. B.; Brown, S. D.; Day, M. W. *Inorg. Chem.* **2001**, *40*, 5083−5091. (c) Pi, C.; Zhang, Z.; Pang, Z.; Zhang, J.; Luo, J.; Chen, Z.; Weng, L.; Zhou, X. *Organometallics* **2007**, *26*, 1934−1946.

DOI: 10.1021/acs.organomet.5b00053
Organometallics 2015, 34, 1354−1363

(d) Betley, T. A.; Qian, B. A.; Peters, J. C. *Inorg. Chem.* **2008**, *47*, 11570−11782. (e) Deraeve, C.; Maraval, A.; Vendier, L.; Faugeroux, V.; Pitie, M.; Meunier, B. *Eur. J. Inorg. Chem.* **2008**, *36*, 5622−5631. (f) Betley, T. A.; Qian, B. A.; Peters, J. C. *Inorg. Chem.* **2008**, *47*, 11570−11582. (g) Malassa, A.; Koch, C.; Stein-Schaller, B.; Gorls, H.; Friedrich, M.; Westerhausen, M. *Inorg. Chim. Acta* **2008**, *361*, 1405−1414. (h) O'Neill, M. K.; Trappey, F. A.; Battle, P.; Boswell, C. L.; Blauch, D. N. *Dalton Trans.* **2009**, 3391−3394. (i) Liu, D.; Cui, D. *Dalton Trans.* **2011**, *40*, 7755−7761. (j) Liu, D.; Luo, Y.; Gao, W.; Cui, D. *Organometallics* **2010**, *29*, 1916−1923.

(4) For examples of polymerization catalysts utilizing quinoline-based ligands, see: (a) Nagy, S.; Krishnamurti, R.; Tyrell, J. A.; Cribbs, L. V.; Cocoman, M. (Occidental Chemical Corporation, USA) Appl.-WO9633202, 1996. (b) Fontaine, P. P.; Kuhlman, R. L. (Dow Global Technologies) Appl. WO2011102990, 2011. (c) Nagy, S.; Winslow, L. N.; Mihan, S.; Chevalier, R.; Lukesova L.; Nifant'ev, I. E.; Ivchenko, P. V. (Equistar Chemicals) Appl. WO2011011040, 2011. (d) Nagy, S.; Winslow, L. N.; Mihan, S.; Chevalier, R.; Lukesova L.; Nifant'ev, I. E.; Ivchenko, P. V.; Lynch, M. W. (EquistarChemicals) Appl. WO2011011041, 2011. (e) Lamberti, M.; Bortoluzzi, M.; Paolucci, G.; Pellecchia, C. *J. Mol. Catal. A: Chem.* **2011**, *351*, 112−119. (f) Nagy, S.; Winslow, L. N.; Mihan, S.; Lukesova, L.; Nifant'ev, I. E.; Ivchenko, P. V.; Bagrov, V. V. (Basell Polyolefine GmbH, Germany) Appl. US20120016092, 2012. (g) Song, S.; Xiao, T.; Wang, L.; Redshaw, C.; Wang, F.; Sun, W.-H. *J. Organomet. Chem.* **2012**, *699*, 8−25.

(5) (a) De Waele, P.; Jazdzewski, B. A.; Klosin, J.; Murray, R. E.; Petersen, J. L.; Theriault, C. N.; Vosejpka, P. C. *Organometallics* **2007**, *26*, 3896−3899. (b) Mashima, K.; Ohnishi, R.; Yamagata, T.; Tsurugi, H. *Chem. Lett.* **2007**, *36*, 1420−1421. (c) Tsurugi, H.; Ohnishi, R.; Kaneko, H.; Panda, T. K.; Mashima, K. *Organometallics* **2009**, *28*, 680−687. (d) Kaneko, H.; Tsurugi, H.; Panda, T. K.; Mashima, K. *Organometallics* **2010**, *29*, 3463−3466. (e) Froese, R. D.; Jazdzewski, B. A.; Klosin, J.; Kuhlman, R. L.; Theriault, C. N.; Welsh, D. M.; Abboud, K. A. *Organometallics* **2011**, *30*, 251−262. (f) Figueroa, R.; Froese, R. D.; He, Y.; Klosin, J.; Theriault, C. N.; Abboud, K. A. *Organometallics* **2011**, *30*, 1695−1709. (g) Fontaine, P. P.; Figueroa, R.; McCann, S. D.; Mort, D.; Klosin, J. *Organometallics* **2013**, *32*, 2963−2972. (h) Klosin, J.; Fontaine, P. P.; Figueroa, R.; McCann, S. D.; Mort, D. *Organometallics* **2013**, *32*, 6488−6499.

(6) (a) Ittel, S. D.; Johnson, L. K.; Brookhart, M. *Chem. Rev.* **2000**, *100*, 1169−1203. (b) Tian, J.; Hustad, P. D.; Coates, G. W. *J. Am. Chem. Soc.* **2001**, *123*, 5134−5135. (c) Bollmann, A.; Blann, K.; Dixon, J. T.; Hess, F. M.; Killian, E.; Maumela, H.; McGuinness, D. S.; Morgan, D. H.; Neveling, A.; Otto, S.; Overett, M.; Slawin, A. M. Z.; Wasserscheid, P.; Kuhlmann, S. *J. Am. Chem. Soc.* **2004**, *126*, 14712−14713. (d) Boussie, T. R.; Diamond, G. M.; Goh, C.; Hall, K. A.; LaPointe, A. M.; Leclerc, M. K.; Murphy, V.; Shoemaker, J. A. W.; Turner, H.; Rosen, R. K.; Stevens, J. C.; Alfano, F.; Busico, V.; Cipullo, R.; Talarico, G. *Angew. Chem., Int. Ed.* **2006**, *45*, 3278−3283. (e) Arriola, D. J.; Carnahan, E. M.; Hustad, P. D.; Kuhlman, R. L.; Wenzel, T. T. *Science* **2006**, *312*, 714−719. (f) Kuhlman, R. L.; Klosin, J. *Macromolecules* **2010**, *43*, 7903−7904.

(7) For selected examples of organometallic additions to quinolines, see: (a) Gilman, H.; Eisch, J.; Soddy, T. S. *J. Am. Chem. Soc.* **1959**, *81*, 4000−4003. (b) Goldstein, S. W.; Dambek, P. J. *Synthesis* **1989**, *3*, 221−222. (c) Rezgui, F.; Mangeney, P.; Alexakis, A. *Tetrahedron Lett.* **1999**, *40*, 6241−6244. (d) Wang, Z.-X.; Li, Y.-X. *Organometallics* **2003**, *22*, 4900−4904. (e) Amiot, F.; Cointeaux, L.; Silve, E. J.; Alexakis, A. *Tetrahedron* **2004**, *60*, 8221−8231.

(8) Belser, P.; Bernhard, S.; Guerig, U. *Tetrahedron* **1996**, *52*, 2937−2944.

(9) Full experimental details are provided in the Supporting Information section.

(10) (a) Pärssinen, A.; Luhtanen, T.; Klinga, M.; Pakkanen, T.; Leskelä, M.; Repo, T. *Eur. J. Inorg. Chem.* **2005**, 2100−2109. (b) Pärssinen, A.; Luhtanen, T.; Klinga, M.; Pakkanen, T.; Leskelä, M.; Repo, T. *Organometallics* **2007**, *26*, 3690−3698.

(11) He, Y.; Qiu, X.; Klosin, J.; Cong, R.; Roof, G.; Redwine, D. *Macromolecules* **2014**, *47*, 3782−3790.

(12) (a) McKnight, A. L.; Waymouth, R. M. *Chem. Rev.* **1998**, *98*, 2587−2598. (b) Wang, W.-J.; Yan, D.; Zhu, S.; Hamielec, A. E. *Macromolecules* **1998**, *31*, 8677−8683. (c) Wang, W.-J.; Kolodka, E.; Zhu, S.; Hamielec, A. E. *J. Polym. Sci. A Polym.* **1999**, *37*, 2949−2957. (d) Dekmezian, A. H.; Soares, J. B. P.; Jiang, P. J.; Garcia-Franco, C. A.; Weng, W. Q.; Fruitwala, H.; Sun, T.; Sarzotti, D. M. *Macromolecules* **2002**, *35*, 9586−9594.

(13) Sheldrick, G. M. *SHELXTL6.1, Crystallographic Software Package*; Bruker AXS, Inc.: Madison, WI, USA, 2008.

DOI: 10.1021/acs.organomet.5b00053
Organometallics 2015, 34, 1354−1363